Molding Innovation

Moldex3D R11
推出全新長纖維
配向預測分析

Moldex3D
MOLDING INNOVATION

Moldex3D R11

推出全新纖維配向預測分析

近年，長纖維複合材料已廣泛應用於汽車、消費性和工業領域。過去常利用玻璃纖維和碳纖維加入塑膠材料，在不顯著增加產品重量下強化機械和熱性能。纖維長度和玻璃纖維強化塑膠的機械性能提升有如圖一所示之關係。雖然加長纖維長度能大幅提升強度與耐衝擊性，然而，這些性能的提升也與纖維的排向有很大的關係。
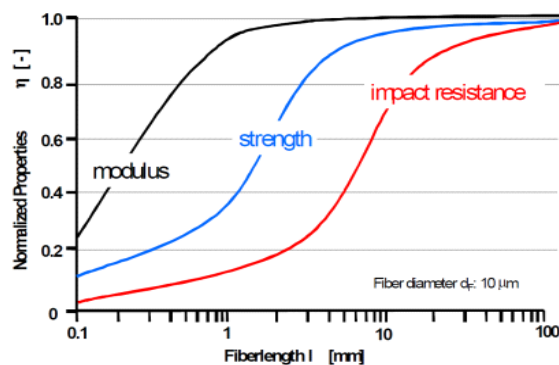
舉例來說，因纖維優選排向，射出成型過程中的剪切流動會使纖維產生配向，造成產品性質的異向性，這多半適合於需要平行流動主軸方向而非垂直方向有較佳強度的產品。但在需要等向性收縮的產品，纖維無特殊配向的隨機分佈有助於避免翹曲。因此對於含纖維材料，為了決定產品性質、協助產品與模具設計、以及選擇加工條件，纖維配向必須被精確的預測。更多詳盡的纖維配向驗證資料收錄在本期電子報的會議論文部分。
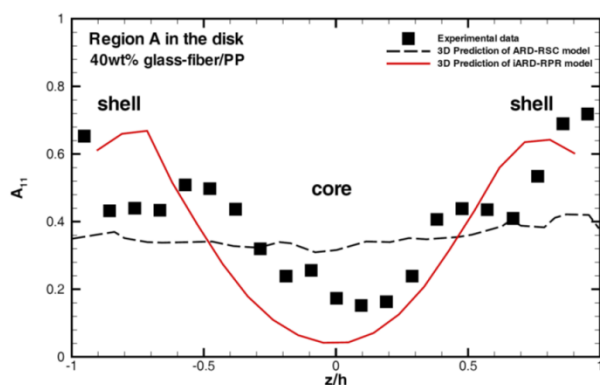

圖一. 複合材料性質隨纖維長度增加而提升 (Source: Plasticomp)

Moldex3D R11 全新長纖配向預測模組，不僅短纖配向，甚至是長纖維也可精確的模擬。傳統纖維配向數學模型是利用由 Folgar-Tucker 推導之非等向旋轉擴散模型(ARD)來描述纖維間干擾，然而此一模型需要五個參數，其計算方式亦不有效率。Moldex3D R11 利用了改良的非等向旋轉擴散模型(iARD)，在預測上大幅領先其他軟體的計算方式，再配合使用延遲主旋轉速率模型(RPR)，iARD 提供了精準的纖維配向預測以及快速計算。

特點包含：

- 只需三個具物理意義的參數，使用者可以輕易設定。
- 加速計算，對於高階四階配向張量計算可加快 50%。
- 不需要設定澆口處的初始配向條件，使用者操作起來更為簡易。
- 模擬長纖特性，包含不同基材、纖維彈性，以及流場影響。
- 更正確的在厚度方向上之纖維配向以及彈性模數分佈。

Moldex3D 的預測正確性可由下圖二所示，利用中央進澆的圓盤試片為測試模型，對於A11張量，越大值代表在流動方向有較佳配向，下圖中實驗數據(方塊)與 Moldex3D iARD 模擬結果(紅色連續線)皆顯示於接近上下表層處(z/h=+-1)有較明顯配向，中心處(z/h=0)則趨於混亂。傳統 ARD 模型無法成功預測此一特性。

Moldex3D 最新長短纖配向預測技術，可協助產品設計和模具開發業者更精準掌控產品品質。更多關於纖維配向的展示與案例，請上網站 http://www.moldex3d.com 來了解更多新功能與應用。

圖二. Moldex3D 的 iARD 長纖預測結果(紅色連續線) 明顯優於傳統 ARD 模型(虛線)，與實驗值吻合

INVESTIGATION OF FIBER ORIENTATION IN FILLING AND PACKING PHASES

Chih-Chung Hsu[1], Dar-Der Hsieh[1], Hsian-Sen Chiu[1], Masashi Yamabe[2]
1. *CoreTech System (Moldex3D) Co., Ltd., ChuPei City, Hsinchu, Taiwan*
2. *Kanazawa Institute of Technology, Ishikawa, Japan*

Abstract

Fiber-reinforced engineering materials are widely used for their superior mechanical properties in lots of plastic parts. And it is truly believed that in the injection molding process the fiber orientation and anisotropy shrinkage are very complex 3D phenomena which may influence the product properties deeply. In this research, the fiber orientation is considered both in filling and packing process numerically. The result of fiber orientation shows a good agreement with experimental data. Moreover, the investigation illustrates the strength of fiber orientation in filling and packing phases with detail.

Introduction

In recent years, the injection molding of fiber-reinforced thermoplastics has been widely used because of their superior mechanical properties in applications. The injection molding of fiber-reinforced composites is a complicated process, where the fiber-induced anisotropic mechanical properties strongly depend on the fiber orientation. The reinforced composites are stronger in the fiber orientation direction and weaker in the transverse direction; the thermal shrinkages are larger in the transverse direction and lower in the fiber orientation direction. In a result, the molded products may have high internal stress and warpage at unexpected locations. Therefore, the design of a new product must take account of processing details.

The flow-induced fiber orientation and anisotropic shrinkages in injection molding are complex 3D behaviors, which makes the properties of injected parts are difficult to be predicted. The direction of fiber orientation is full 3D components, which makes it difficult to study by the traditional 2.5D model. Thus, a true 3D injection molding simulation technique is therefore employed for obtaining the 3D distribution of fiber orientation in this study. For validation purpose, a ribbed flat plate with side gate positions is conducted by experiment to examine the effect of fibers in filling and packing process. Moreover, the anisotropic warpage behavior is also being discussed.

Governing equations

The polymer melt is assumed to behave as Generalized Newtonian Fluid (GNF). Hence the governing equations to simulate transient, non-isothermal 3D flow motion are shown as following:

$$\frac{\partial \rho}{\partial t} + \nabla \cdot \rho \mathbf{u} = 0 \tag{1}$$

$$\frac{\partial}{\partial t}(\rho \mathbf{u}) + \nabla \cdot (\rho \mathbf{u}\mathbf{u} - \boldsymbol{\sigma}) = \rho \mathbf{g} \tag{2}$$

$$\boldsymbol{\sigma} = -p\mathbf{I} + \eta(\nabla \mathbf{u} + \nabla \mathbf{u}^T) \tag{3}$$

$$\rho C_P\left(\frac{\partial T}{\partial t} + \mathbf{u} \cdot \nabla T\right) = \nabla(\mathbf{k}\nabla T) + \eta \dot{\gamma}^2 \tag{4}$$

where $\mathbf{u}$ is the velocity vector, T the temperature, t the time, p the pressure, $\boldsymbol{\sigma}$ the total stress tensor, ρ the density, η the viscosity, k the thermal conductivity, C_p the specific heat and $\dot{\gamma}$ the shear rate. The FVM due to its robustness and efficiency is employed in this study to solve the transient flow field in complex three-dimensional geometry.

Fiber orientation

The fiber orientation state at each point in the part is represented by a 2nd-order orientation vector A, where

$$A_{ij} = \int (p_i p_j)\varphi(p)dp \tag{5}$$

The equation of orientation change for the orientation tensor proposed by Advani and Tucker is employed for the analysis:

$$\frac{\partial A_{ij}}{\partial t} + u_k \frac{\partial A_{ij}}{\partial x_k} = A_{ik}\Omega_{kj} - \Omega_{ik}A_{kj} + \\ \lambda(A_{ik}E_{kj} + E_{ik}A_{kj} - 2A_{ijkl}E_{kl}) + 2C_I\dot{\gamma}(\delta_{ij} - 3A_{ij}) \tag{6}$$

Where C_I is the interaction coefficient with the value ranged from 10^{-2} to 10^{-3}. In this study, we take C_I as 10^{-2} for default value. For the fourth-order tensor A_{ijkl}, a closure approximation is needed in order to calculate the distribution of 2nd order A on the basis of a velocity field. Here, the hybrid closure approximation will be primarily adopted.

Implementation details

The fiber-reinforced plastic material adopted in this study is DURANEX®3300(Grade name, written as PBT-GF in the following description). The molding condition is tabulated in Table 1. The geometry model

is a ribbed flat plate with side gate positions, which is shown as Fig.1. The geometry model used to conduct the experiments is the same mold with side gate respectively. The node positions for measuring warpage behavior are illustrated in Fig. 2. The measurement results of deformation on these nodes are used to compare to simulation results. Furthermore, in order to observe the fiber orientation, the mold is divided into 20 layers in the experiment in the thickness direction, while the corresponding displayed layer number by simulation is 10. The schematic diagrams of fiber orientation for each layer using in the simulation are shown as Fig. 3 and 4.

Results and Discussions

In convenience to show the comparison of fiber orientation between experiment and simulation results, the orientation of the lines indicates the most favorable orientation direction, and the displayed color represents the degree of orientation. To clarify the fiber orientation inside the cavity, position 1~3 is investigated by three cutting plane: front, middle and back, and position 4 is done by left, center and right planes. Fig. 5~8 shows the comparison of fiber orientation between experiment and simulation results. Moreover, the simulation results in filling and packing process are also illustrated.

For observed positions 1 and 2 in Fig. 5 and 6, the evolution of fiber orientation is predicted well qualitatively as experimental result both in filling and packing process. We can see that due to the cooling effect in packing process, the polymer has solidified that there is little changes in fiber orientation. As for the front and back plane near the mold wall, the shearing flow tends to align the fibers along the flow direction. While the situation is different in the middle plane, the flow is shear free or lower and the fiber orientation no longer aligns the flow direction. Some even aligns perpendicular to the flow direction in the vicinity of the melt entrance region. However, as the melt starts developing flow pattern, the fiber continues to align to the specific directions under the effect of shear rate. This is obviously predicted as Fig. 5-(b) for distinct behavior in filling and packing process.

For observed position 3, Fig. 7 shows the fiber orientation in the end of flow line. There is some strength and direction difference in filling and packing phase. However, packing phase predicts better than filling in the phenomena that fibers tend to flip over and stand in the observed slicing plane. Observed position 4 as showing in Fig. 8 is taken to investigate the fiber orientation in the thickness direction. A simple sketch map of fiber orientation can be formed as Fig. 9. We can divide the fiber orientation distribution into three laminates, where zone A is the outermost skin with no distinct pattern of orientation. Zone B exposed the high shear rate that the fiber oriented in direction of flow. In the inner laminate zone C, medium shear rate or low

shear rate may result in little orientation and even transverse to flow direction. Fig. 9 is typical in injection-molded part and can be predicted by the present analysis.

In Fig. 10, we show the numerical and experimental warpage measurement. The figure show that the trend of deformation on the nodes is in a good agreement with both experiment and simulation. Since the displacement strongly depends on the strength of fiber, an uneven distribution of fiber orientation due to flow pattern may lead the mechanical properties to be anisotropic.

Conclusions

In this research, the numerical algorithm to simulate fiber orientation is validated with corresponding experimental measurements. A ribbed flat plate with side gate is used as test models, and the comparison of the slicing fiber orientation between simulation and experiment results is in a good agreement. It is found that due to the growing layer of solidified polymer during the packing process, the fiber orientation behaves a little differently in the strength of magnitude and still keeps generally the same distribution as filling process. With the consideration of fiber orientation in packing process, the product property during the whole injection molding process is assured more. Moreover, the predicted warpage deformation values are being obtained with reasonable comparison with the experimental data under the considering of fiber orientation both in filling and packing process.

Reference

1. Michii Takayuki, Seto Masahiro, Yamabe Masashi, and Otsuka Hiroki, "Warpage Mechanism duo to Fiber Orientation during Injection Molding", 467, Seikei-Kakou, Vol.**16**, No.7, (2004).
2. W.H.Yang, David C. Hsu, Venny Yang and R. Y. Chang, "Computer Simulation of 3D Short Fiber Orientation in Injection Molding", 470, ANTEC 2003, Nashville, (2003)
3. R. Y. Chang, W. S. Yang, "Numerical Simulation of Mold Filling in Injection Molding Using a Three-Dimensional Finite Volume Approach.", 125, Int. J. Num. Meth. Fluids, Vol. **37**, (2001).

Table 1 Molding conditions

Melt temperature ($^\circ C$)	250
Mold temperature ($^\circ C$)	60
Injection velocity (m/min)	1.0
Holding pressure (MPa)	68.6
Injection time + Holding time (sec)	10
Cooling time (sec)	20
Cycle time (sec)	40
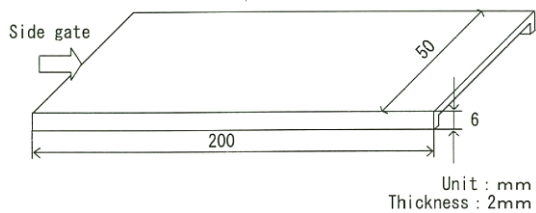
Fig.1 Geometry of mold cavity
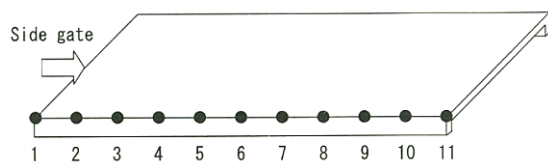
Fig.2 Measuring nodes for warpage behavior

Fig. 3 Observation Position
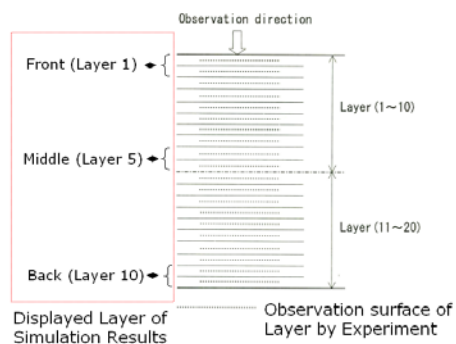
Fig. 4 Observation layers by experiment and corresponding layers by simulation.
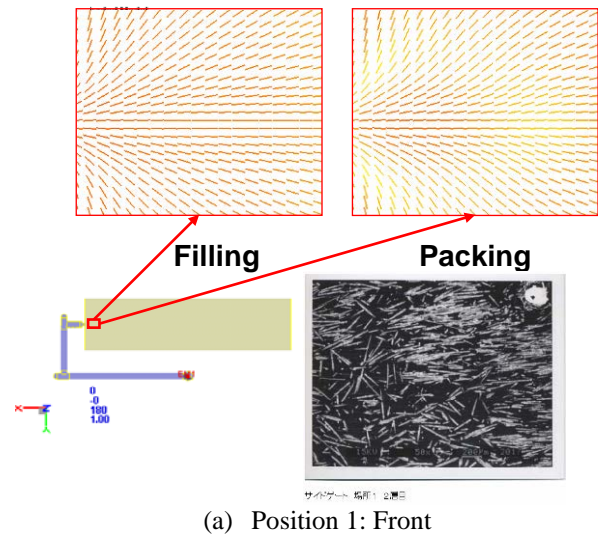
(a) Position 1: Front
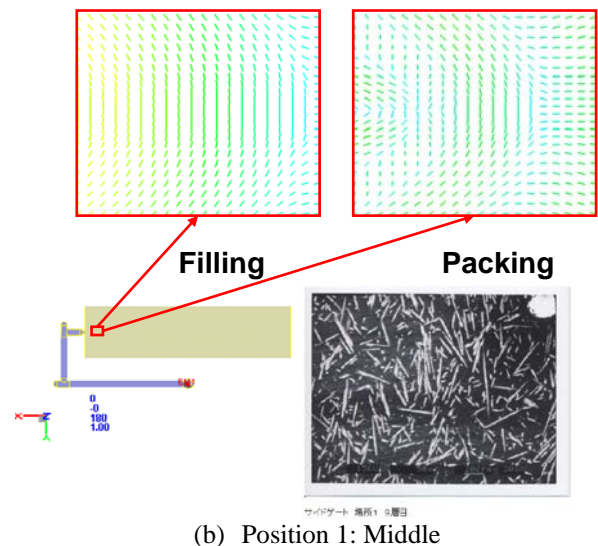
(b) Position 1: Middle
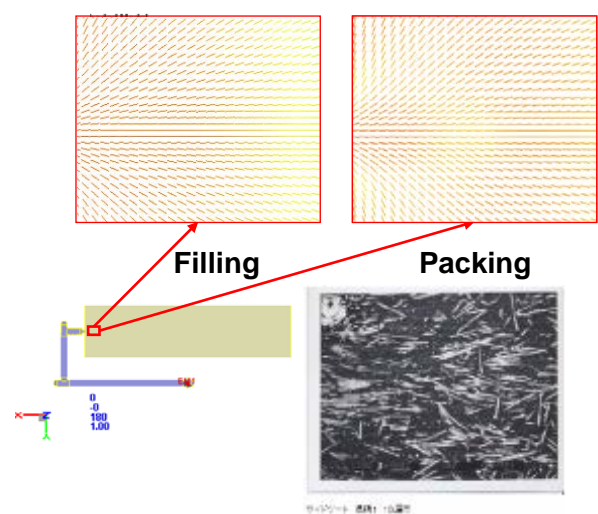
(c) Position 1: Back

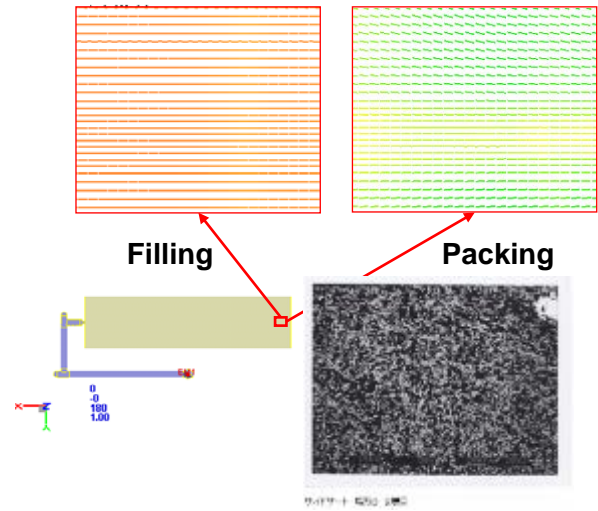**Fig. 5** Fiber orientation comparison for Position 1
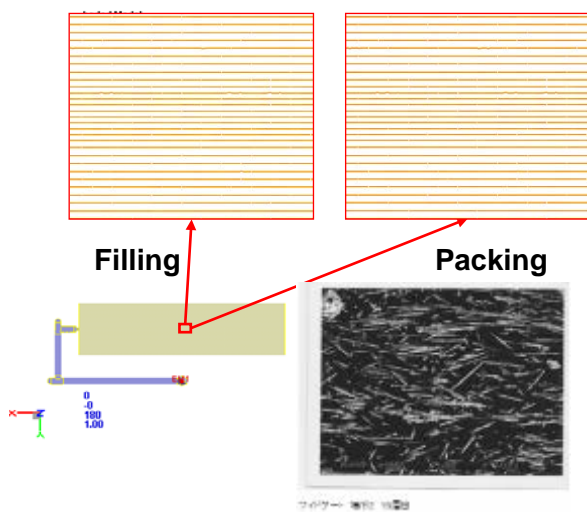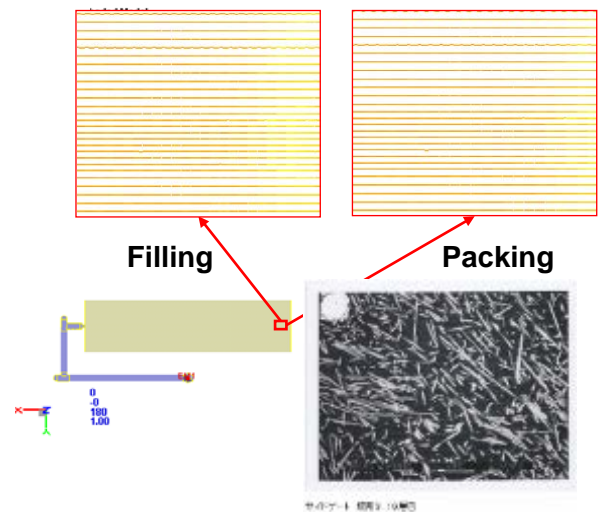
(a) Position 2: Front

(b) Position 2: Middle

(c) Position 2: Back

Fig. 6 Fiber orientation comparison for Position 2
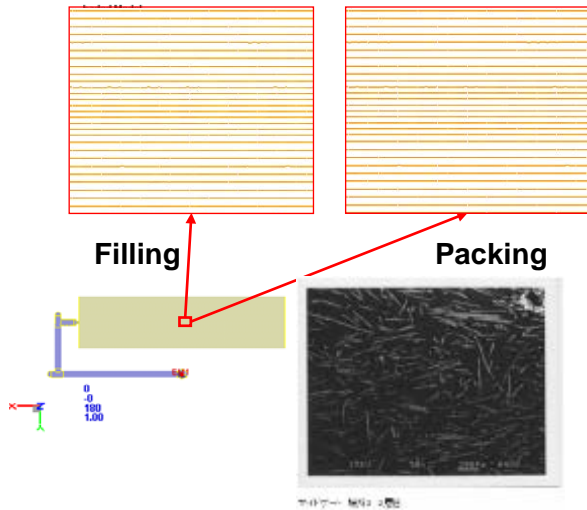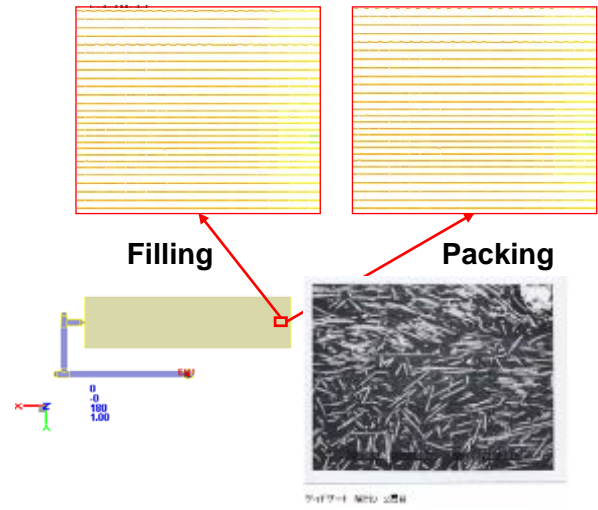
(a) Position 3: Front

(b) Position 3: Middle

(c) Position 3: Back

Fig. 7 Fiber orientation comparison for Position 3

Filling

Packing

(a)   Position 4: Left

Filling

Packing
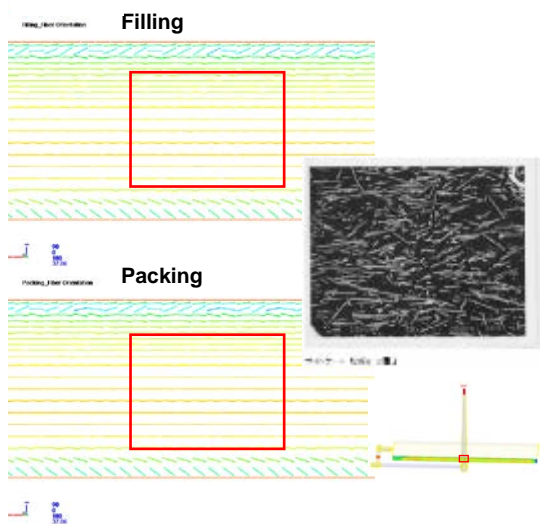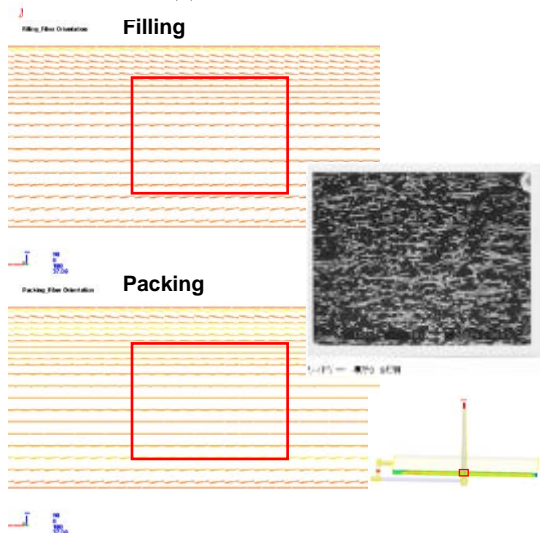
(b)   Position 4: Center

Filling

Packing
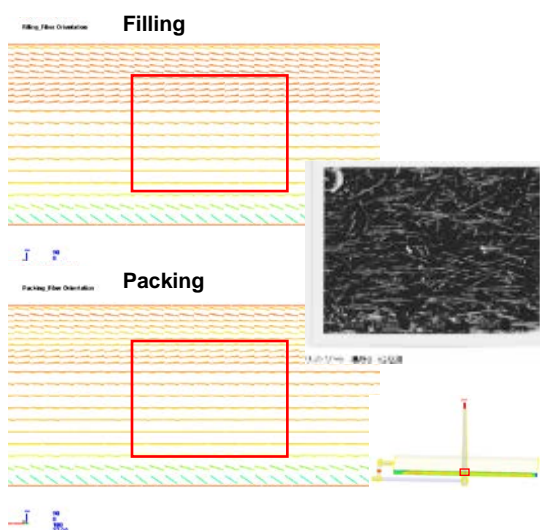
(c)   Position 4: Right

Fig. 8 Fiber orientation comparison for Position 4
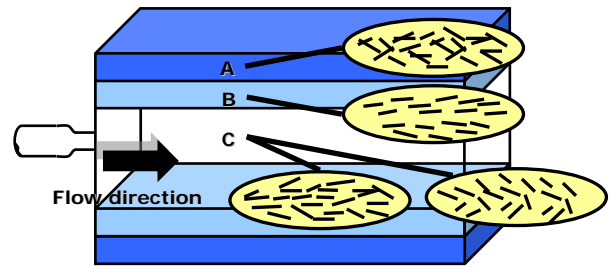

Flow direction

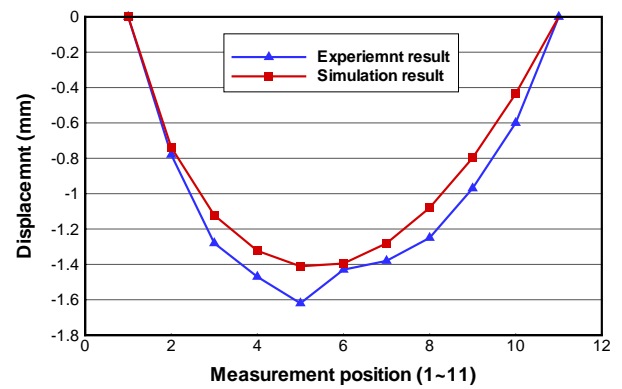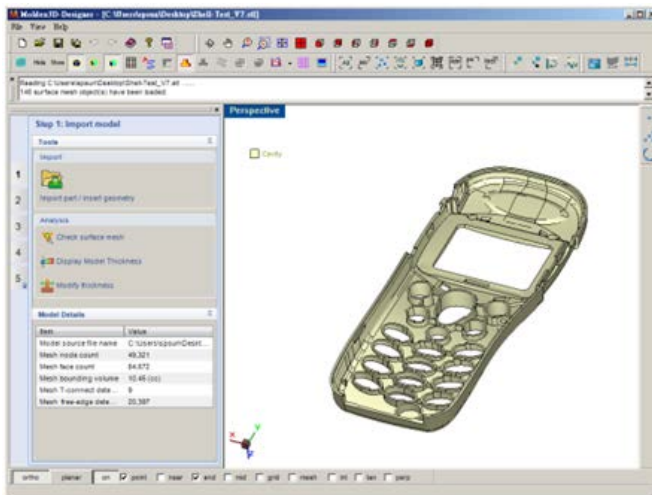**Fig. 9** Simple sketch map of fiber orientation

Fig. 10 The comparison of deformation between experiment and simulation results

全新 Moldex3D R11.0 輕鬆達成厚度修改

除了 eDesignSYNC 能提供 eDesign 和 CAD 整合介面之外，現在 eDesign 也可以進行簡易模型修改。 全新的厚度修改 (Modify Thickness)功能，方便使用者在 eDesign 的環境下，迅速進行模型修改。如果使用者不確定厚度修改帶來的影響，可以進行多次模擬並從中選出最佳的結果。厚度修改功能使用步驟如下：
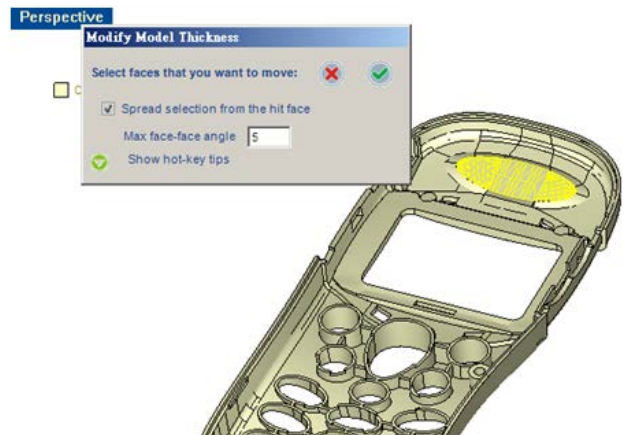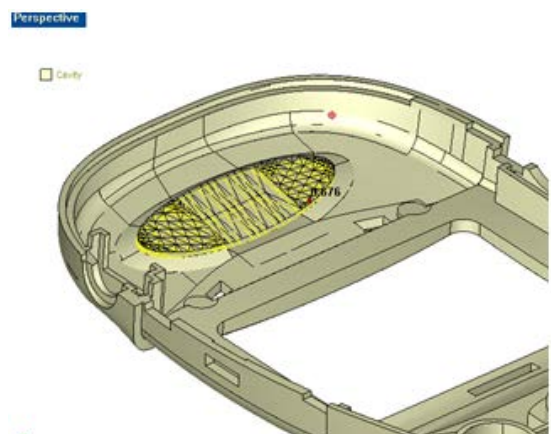
1. 匯入模型

2. 在 Analysis 功能欄中可以選取新的 Modify thickness 功能

3. 點選後，Modify Model Thickness 功能即會出現

4. 點選欲修改厚度的表面，可以輸入或拖曳至理想厚度值，在這裡我們將厚度修改至 0.67mm

5. 全新 Designer 功能，讓您在 eDesign 環境下，也能隨時都能完成厚度修改
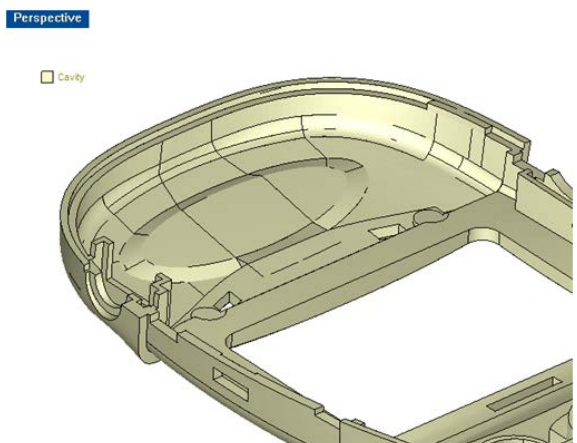
讓 eDesignSYNC 牽線 完美結合 CAE 和 CAD
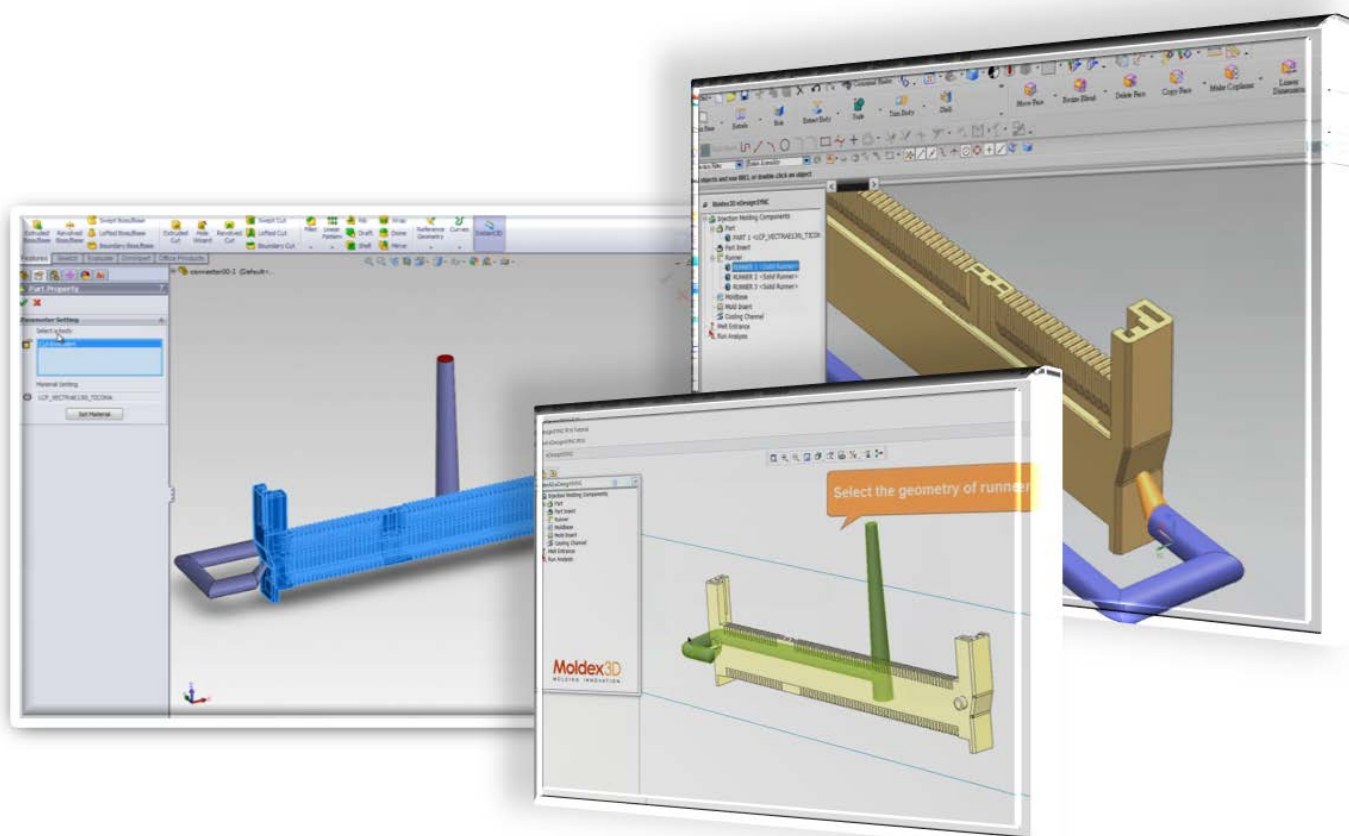
Moldex3D eDesignSYNC 是一款能讓 CAE 和 CAD 軟體，如： NX, Creo 和 SolidWorks 完美結合的套件。 透過人性化的使用介面和全自動 3D 網格技術，eDesignSYNC 輕鬆簡化模擬分析的前處理過程。使用者可以在 CAD 環境介面中，即完成設定每個製成參數和前處理。eDesignSYNC 可以提供流動、保壓、冷卻、翹曲、多材質和纖維…等分析。

欲知道更多關於 eDesignSYNC 在 CAD 環境下使用的實例，請點選這裡觀看基本教學和案例分析影片。

基本教學
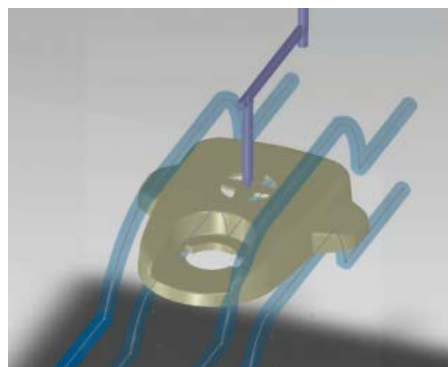
從以下影片，使用者將可以了解 eDesignSYNC 的基本操作。迅速完成精準模流分析。

› **選擇您的 CAD 軟體並觀看影片：**
  NX   Creo   SolidWork

實體流道和對稱運算

eDesignSYNC 可以支援流道系統- 有了實體流道之後，使用者可以在模型上進行對稱運算，不僅可以降低運送時間，同時可以提升模擬精確度。

› **選擇您的 CAD 軟體並觀看影片：**

NX　　Creo　　SolidWorks

案例分析

使用 eDesignSYNC 可以降低設計成本，透過這些案例解說，使用者可以了解如何使用 eDesignSYNC 協助改善製程中的缺陷。

連結器

在這個案例中，我們將使用 eDesignSYNC 對連接器進行模流分析。從分析的結果，我們可以輕易發現材料不平衡的流動模式。經過修改連結器的另一面厚度後，成功改善了模流分析結果。

› **選擇您的 CAD 軟體並觀看影片：**

NX　　Creo　　SolidWorks

東陽用模流分析建構全球競爭優勢

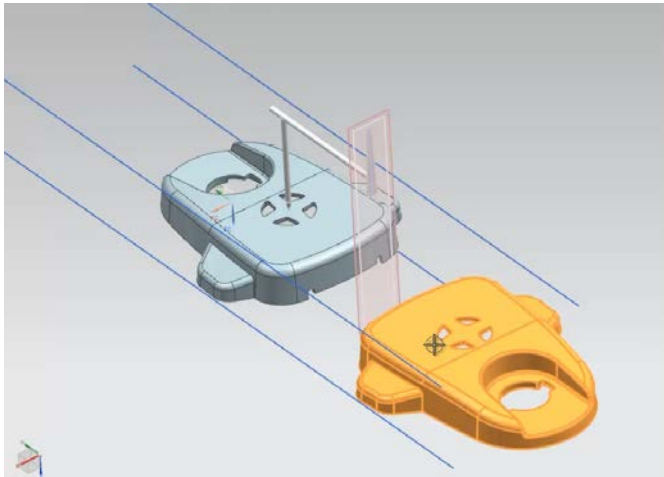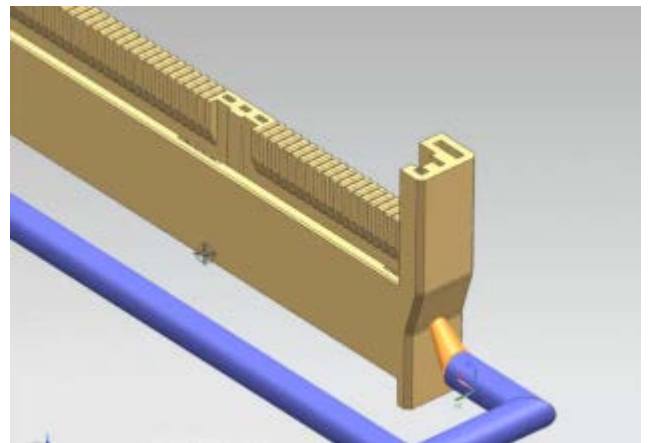東陽實業廠成立於 1967 年，是一家歷史悠久、品質卓著的汽車零配件專業供應廠。主要的產品涵蓋各式汽車外裝重要零件前後保險桿、水箱護罩、門邊飾板...等，以及重要的內裝件儀表板、中央扶手、門板..等。2011 年全球營業額超過十億美金，員工人數超過 7200 人，業務範圍涵蓋 OEM 與 AM 二種市場。

東陽實業廠的 OEM 事業部參與世界一流車廠的協同設計，自造型階段開始，對車廠所提供造型與 3D 數據進行 LAYOUT 與製造可行性評估，提出潛在問題的改善方案，取得客戶認可後再進行細部設計與模流分析。由於汽車的內裝與外裝產品是用車人視覺的焦點，外觀品質的好壞非常重要，凹痕(sink mark)、縫合線(weld line)、變形與間隙段差不均等現象，均令客戶無法接受。

然而，全球車廠競爭激烈，在樣多量少環境下，各車廠無不在外觀造型上做區隔，以吸引消費者的青睞；保險桿、前欄、空氣動力套件等外觀塑膠製品通常是改變的優先對象。同時，東陽也必須面對來自中國大陸、印度的低價汽車零組件市場發展與競爭。過去東陽大多採用傳統的試誤手法來找出及修正問題點，花費許多時間和成本；面對外部競爭者、客戶對品質與成本的要求，需提昇開發能力。

東陽自 2000 年起導入 Moldex3D 電腦輔助分析，應用於產品開發。由於成效卓著，逐年擴大 CAE 的使用項目，目前共計有 13 套 Moldex3D 用於產品設計、模具設計部門及外部供應商：

> 協助設計人員了解產品幾何、模具、材料與成型條件之關聯性。
> 降低開發成本。
> 作為經驗學習、建立產品與模具設計基準。

由分析結果求得最適模具設計方案，訂定基準書供成本估算與模具驗收。在模具製作過程，依基準書比對模具差異，確保分析方案與實際相符，以利試模對策時間縮短。利用 Moldex3D 在產品設計與模具開發階段預測產品可能發生包封問題（圖(a)），可以在包封位置增加頂針，由頂針位置排氣(圖(b))；或是改變進澆位置避免包封產生。在試作階段，設計與開發等相關人員進行結果比對，有助於模具修改對策的正確性與時間，並可以進而累積經驗，充實設計知識庫。

東陽 OEM 事業群製造部簡志富協理表示：「科盛科技不僅是一個模流軟體供應商，也真正了解我們所面臨的成型挑戰，總是能提供我們最即時的專業協助。」。透過持續的設計流程改善、保險桿類等大型產品成型週期平均減少了 21.7 秒，其他各類產品也明顯縮短了成型週期。「這些成型週期的縮減，等於我們公司的產能提升 21.28%，大大提昇了成本競爭力，我們將在設計的更上游就採用模流分析，朝向同步設計與優化邁進。」簡協理微笑且自信地下了這個小結論，心中也對集團的 CAE 規劃有了下一個階段的藍圖。
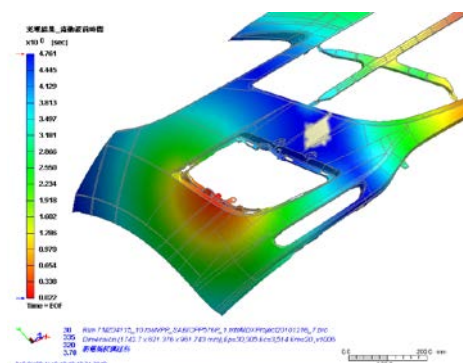
a. 模擬預測包封位置
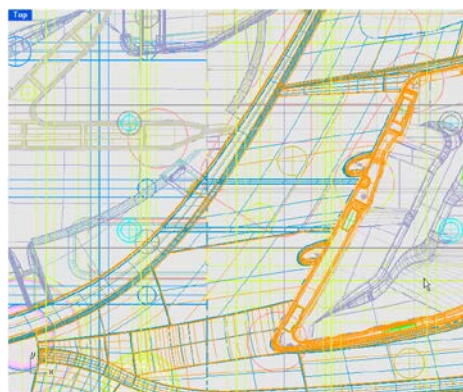
b. 拆模時預先在模具安置頂針以便排氣

UTAC 成功應用 Moldex3D 封裝模流分析技術，榮獲第 44 屆 IMAPS 國際論文獎

UTAC 為全球知名的獨立半導體封測供應商，提供客戶完整的封裝和測試服務、工程和製造服務以及解決方案。

微小化是當前 IC 封裝產業所面臨的挑戰。因為覆晶封裝擁有高輸入/輸出(I/O)介面、高效能和小型化，廣受產業界採用。雖然覆晶技術有許多優於其他高密度電子封裝方法的優勢，在確保成型性和降低成型缺陷方面，卻遭遇許多困難，如：降低接點間隔、平衡支座高度、更輕薄封裝以及模壓底膠封裝材料的特性等等。

這些因素潛在的交互作用以及對於封裝良率、可靠度和效能的影響，大幅增加技術難度。包封問題也因為在晶片下方接點區域的微小間隙而面臨更多挑戰，如：流動不平衡以及流阻情形。

自 2009 年起，UTAC 開始應用 Moldex3D 於虛擬試模實驗，已成功使用該軟體完成數項封裝專案。Moldex3D 模擬功效讓我們成功解決製程中關鍵問題" 團隊負責人 Ore Siew Hoon 說道。" 以往，解決封裝成型問題常常會動用到大型的實驗設計矩陣，因為液體流動、熱傳遞和封膠聚合物複雜的交互作用，使得製程實驗既耗時又困難。但是數值模擬卻對於分析複雜的物理現象十分有效。" 最近 UTAC 在模壓覆晶封裝方面的研究成果榮獲第四十四屆 IMAPS 國際微電子與構裝學會最佳論文。關於論文詳情，請點此閱讀。
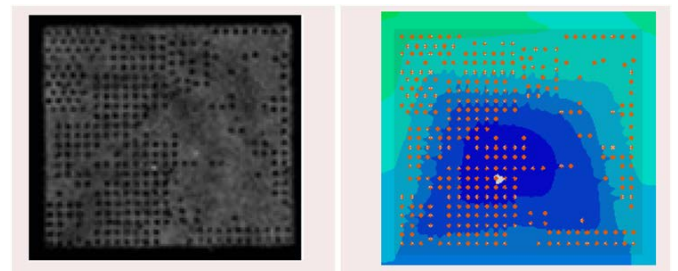
Moldex3D 能精準預測模壓底膠封裝過程中常見的包封缺陷

Molding Flow Modeling and Experimental Study on Void Control for Flip Chip Package Panel Molding with Molded Underfill Technology

Jonathan Tamil[1], Siew Hoon Ore[2], Kian Yeow Gan[3], Yang Yong Bo[4], Geraldine Ng[5], Park Teck Wah[6],
Dr Nathapong Suthiwongsunthorn[7], Dr Surasit Chungpaiboonpatana[8]
United Test and Assembly Center[1,2,3,4,5,6,7,8], 5 Serangoon North Ave 5 S554916,
Jonathan_Tamil@sg.utacgroup.com[1], (65) 65511386[1]

Abstract

Increasing challenges are faced to ensure moldability with rapid advances in flip chip technology such as decreasing bump pitch and stand-off height, especially when commercial Moldable Underfill (MUF) is used and in particular, during panel level molding. One key challenge faced is severe void entrapment under the die. Experiments involving a large DOE matrix, which require significant time and process resources, are typically used to solve this issue. 3D flow simulation can be used to optimize the process to reduce defects without doing actual runs. Mold flow simulation can effectively reduce the design-to-implementation cycle time, identifying key problems before actual fabrication. In this paper, 3D mold flow simulation using Moldex3D™ V10 is applied to transfer molding to optimize design and process parameters.

This paper proposes and verifies a systematic method that can save computational resources by using 2 steps analysis: simplified panel simulation and single package simulation. The initial step, simplified panel level simulation, is to optimize the process parameters to obtain balanced melt front. The second step is to study on the package level the effect of various package-scale parameters. This analysis provides a prediction of the void location and an insight on the appropriate parameters to minimize void problem. The actual voids location and size from the experiment was captured by SAT machine and short shots were obtained. For final validation, a complete panel-level flow model is built, where the process and design parameters adopted in the actual molding were implemented. The mold filling simulation showed good correlation with the experimental short shots and actual void location. With optimized parameters from the simulation used as guidelines, experimental tests were conducted and the study showed that the simulation is a useful tool to optimize the molding process.

1. Introduction

Flip-chip packages have gained significant use in production over the years because of its high inputs/outputs (I/O), enhanced performance and small form factors[1]. Though the flip-chip technology has various advantages over the other high-density electronic packaging approaches, there are rising challenges to ensure moldability and mimimize defects with rapid advances in flip chip technology such as decreasing bump pitch, stand-off height, thinner package profiles and moldable underfill (MUF) materials. The complexity was further exacerbated by the possible interactions between these factors and their impact on package yield, reliability and performance.

Transfer molding process using MUF for flip-chip devices was developed due to reduction of process steps, cycle time and cost compared with the conventional capillary underfill process. But void entrapment[2] challenges are faced with increasingly small gap at the bumps area under the die, resulting in significant melt front imbalance and flow resistance.

Experiments involving a large DOE matrix are typically used to solve this issue. However, applying the conventional trial-and-error method to optimize this process is time consuming and difficult because of the complex interactions between fluid flow, heat transfer and polymerization of MUF. Hence computer-aided-engineering (CAE) is an effective tool for analyzing the complicated physical phenomena inherent in the process of encapsulation of flip chip packages. Simulation can be used to provide further insights of the underlying physics to help address the defect concerns.

In this paper, 3D mold flow modeling of the transfer molding process with MUF using Moldex3D V10 is applied to optimize design and process parameters that can reduce device defects and enhance yield. The Cross Castro-Macosko model is used to define the MUF epoxy viscosity behaviors, where its rheological parameters were acquired using parallel plate rheometer and DSC(Differential Scanning Caloriemeter). The test vehicle selected is a flip chip package with bump height of 100um.

A systematic approach is developed to address the complex flow issues. As the full panel bumped array of flip chip devices would require high computational resources and time, an initial simplified chip level simulation is used to study the effect of various parameters. This analysis provides a prediction of the void location and an insight on the appropriate parameters to minimize void problem. With the insights provided by the preliminary study, the full panel level study is conducted next to evaluate the impact of process and design parameters with the aim of obtaining a balanced melt front and minimize voids.

The actual voids location and size from the experiment was captured by SAT machine and short shots were obtained. The mold filling simulation showed good correlation of the mold fronts obtained by process short shots and actual void locations. With the successful validation of the simulation, the simulation matrix as shown in Fig.1 was designed for a comprehensive assessment of the process, design and material impact on the molding performance.

Geometry	Process	Material
• Bump pitch • Bump height • Bump diameter • Package size • Die size • Die thickness • Bump population	• Mold temperature • Transfer profile • Filling time • Preheat time • Transfer pressure	• Reactive viscosity • Curing kinetics • Gel time

Fig.1: Rheokinetic Flow Modeling Matrix

From the rheokinetic flow modeling of MUF process, we identified the key factors and minor factors on void trapping simulation results from the extensive list of process, design and material parameters. This paper presents the valuable insights of various factors on flip chip device moldability based on process and materials used for the device. The insights can be used as upfront guidelines to predict and reduce potential product defects and failures.

With consideration of process, materials and design, this study has demonstrated that mold flow simulation is an effective tool to reduce the design-to-implementation cycle time with identification of potential void and melt front imbalance issues before actual fabrication. The simulation tool is used actively to-fro in conjunction with materials, process and design inputs and considerations, to predict the trend of various factors on moldability upfront to reduce the yield, cost and cycle time as shown in Fig.2. With our increasing range of flip chip products provided, we provide a comprehensive closed-loop solution including moldflow, thermal, mechanical and electrical studies[3] to the rising challenges faced with greater consumer demands for smaller and thinner flip-chip packages with better performance and greater functionalities.
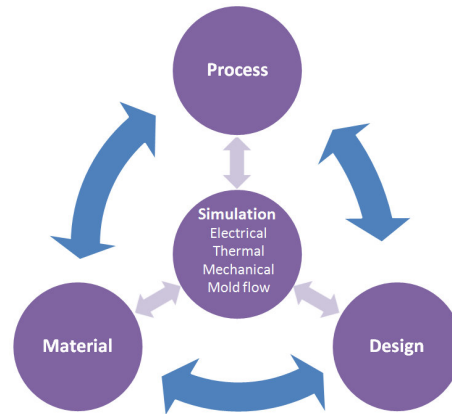

Fig.2: Closed-Loop Material, Process, Design and Simulation to Enhance Flip Chip Product Yield and Reduce Cycle Time

2. Rheokinetic Characterization of Moldable Underfill

In the transfer molding process, flow and heat transfer is dynamically coupled with the curing reaction[4]. The kinetics of the curing reaction not only affects the degree of conversion of the molding compound but also has strong effort on the mold flow with increase in viscosity due to curing reaction. Viscosity is influenced also primarily by temperature and shear rate. Therefore the rheological behavior of molding compounds is of fundamental importance for modeling of the molding process.

The MUF rheokinetic behaviors and other material properties were characterized for the flow modeling, including viscosity with varying shear rates and temperatures, curing kinetics, thermal conductivity, heat capacity and mechanical properties etc. The curing kinetics were measured using DSC with at different temperature ramp-up rates (5, 10, 20, 40°C/min). The experimental data of cure conversions were fitted by numerical parameters using the Kamal's relation [5][6] and the fitting parameters are summarized in Table I for MUF sample A. The experimental data and the numerical fitting line show good agreement, as shown in Figure 3.

$$\frac{d\alpha}{dt} = \left(k_1 + k_2 \alpha^m\right)\left(1 - \alpha\right)^n$$

$$k_1 = A_1 \exp\left(-\frac{E_1}{RT}\right)$$

$$k_2 = A_2 \exp\left(-\frac{E_2}{RT}\right)$$

Parameter of Kinetics	Unit	Value
M	N/A	5.0467 e-1
N	N/A	1.0207
A	1/sec	1.7751 e+3
B	1/sec	1.7746 e+5
T_a	K	7.0369 e+3
T_b	K	7.0372 e+3

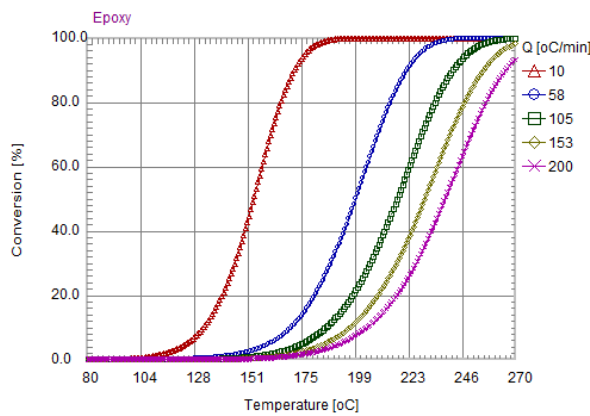Table 1. Numerical parameters using the Kamal's relation and the fitting parameters for MUF sample A

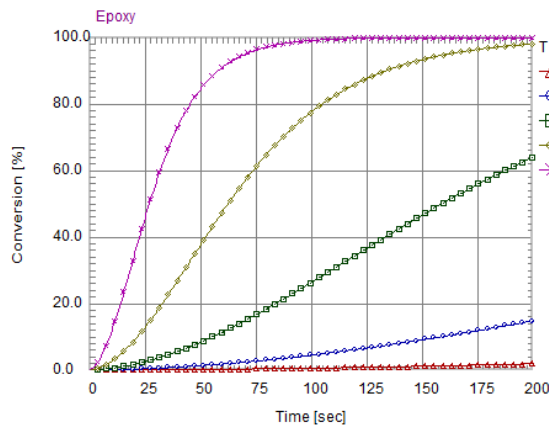Fig 3. Curing Kinetics Curves:
Conversion (%) vs Temperature

Fig 4. Curing Kinetics Curves:
Conversion (%) vs Time

The viscosity is measured by the parallel plates rheometer at different temperatures ramping rates (10, 20, 40, 60 °C/min) and different shear rates (1, 2.5, 5, 10 1/s), where the viscosity changes with time. The measured viscosity is fitted by the following Cross Castro Macosko's model [7]. The experimental data set and numerical fitting results with good agreement is shown in Fig 4 and 5.

$$\eta = \frac{\eta_0}{1 + \left(\dfrac{\eta_0 \gamma}{\tau^*}\right)^{1-n}} \left(\frac{\alpha_g}{\alpha_g - \alpha}\right)^{c_1 + c_2 \alpha}$$

$$\eta_0 = B e^{\frac{T_b}{T}}$$

	Unit	Value
n		9.683 e-2
Tau*	Dyne/cm^2	2.000 e+3
B	g/cm.sec	6.263 e-43
T_b	K	4.937 e+4
C_1		1.818
C_2		-5.521
α_g		0.25

Table 2. Numerical parameters for Cross Castro Macosko model

Where γ is shear rate, α is conversion, n is the power law index, η_0 the zero shear viscosity, τ^* is the parameter that describes the transition region between zero shear rate and the power law region of the viscosity curve.
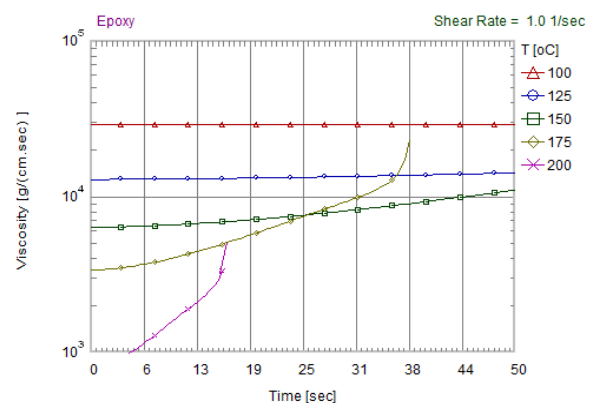

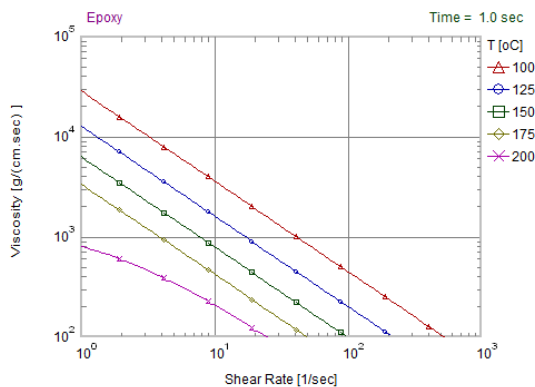Fig 5. Viscosity Curves:
Viscosity vs Time

Fig 5. Viscosity Curves:
Viscosity vs shear rate

3. MUF Flow Modeling and Experimental Benchmarking

Results for Flip-chip Test Vehicle

An illustration of the transfer molding of the selected flip chip device for our current study is shown in Fig.6. The die thickness (Dt) is 0.15mm, underfill gap between substrate and die (Bh) is only 0.1mm and total mold height (Mt) is 0.53mm. There are minimum 3 mesh elements between the smallest gaps in the model. The transfer time with optimum ram speed profile control was obtained from the mold process DOE. The transfer molding process simulation is conducted using Moldex3D module for IC molding process. Actual experimental data are used in order to benchmark with our MUF flip chip transfer molding modeling.
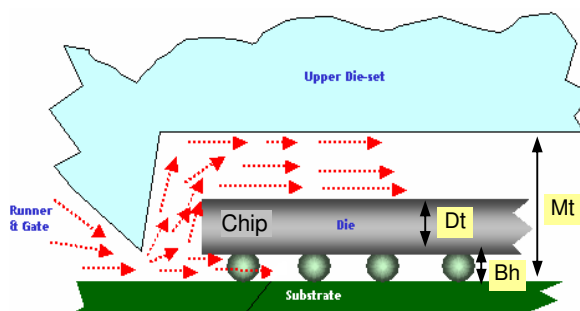
Fig. 6 Transfer molding of the selected flip chip device

The experimental short shots and simulation results are compared to assess the melt front predictions. Table 2 shows the short shots of the mold process results captured during the mold process. The comparison showed good correlation of the melt fronts obtained by process short shots with the mold filling simulation, where the melt front advancement patterns are similar to the simulated melt front contours. The melt front as observed from both short shots and simulations is generally balanced, except for slight flow retardation observed on the die areas due to flow resistance from the narrow flow channels created by the narrow gaps in these areas above the under the dies.

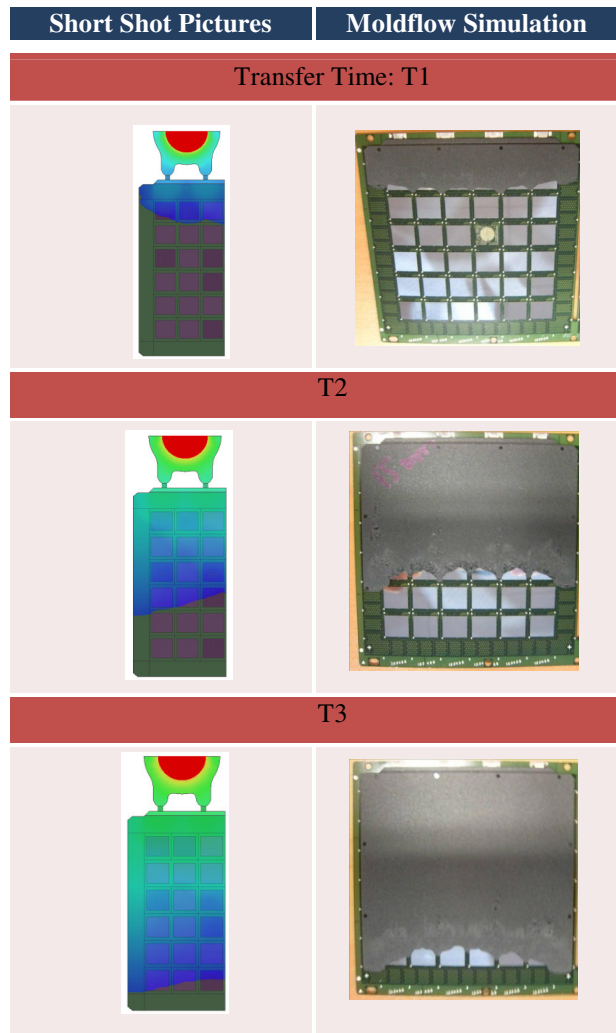| Short Shot Pictures	Moldflow Simulation
Transfer Time: T1	
T2	
T3	

Table 2: Short Shots and
Melt Front Simulations Correlation

The actual voids location and size from the experiment was captured by scanning acoustic microscope (SAT) imaging machine. We can observe the entrapped voids in the underfill areas in selected packages on the different rows in the panel as shown in Table 3. The locations of the simulated and experimental void entraps are nearly identical. Thus the simulation showed good correlation of the actual void locations.
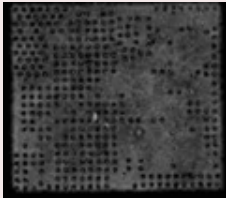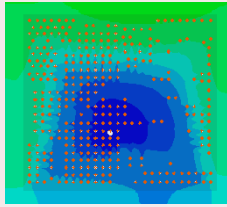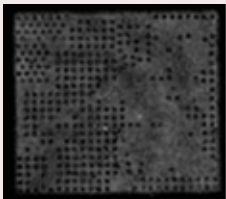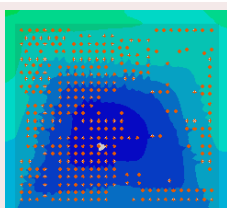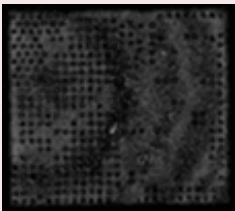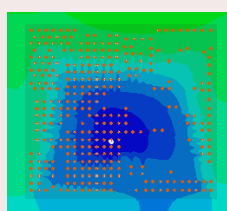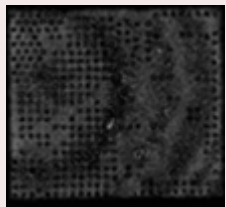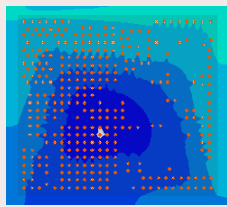
Voids by SAT	Moldflow Simulation
Row 1	
Row 2	
Row 3	
Row 4	

Table 2: Short Shots and
Melt Front Simulations Correlation

Fig.7 shows the simulated melt front advancement contour results for both above and under the die with the flip chip bumps. Initially, the melt front of the mold top side and bottom side are similar, but due to the presence of bumps, the melt fronts above and underneath the die are separated. The melt front near the top side of mold cavity is much faster than that of the bump area of near the substrate side where the 100μm gap is much narrower than the 280μm For this test vehicle, it is observed that the void trapping phenomena is more severe under the more densely bumped area which are next to the much less densely bumped area. The flow imbalances due to the above factors

are observed to be key factors of void trapping where the two separated melt fronts are merged again.
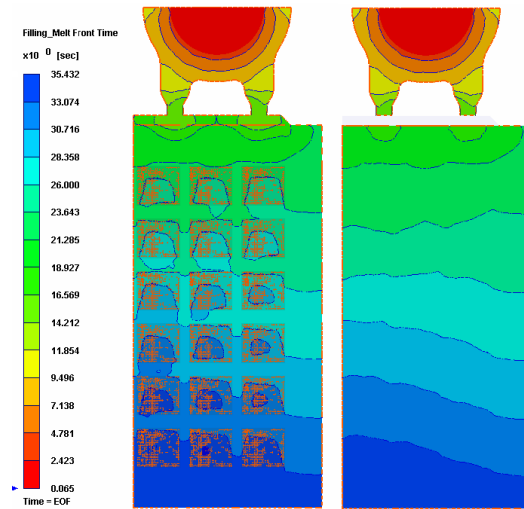

Fig. 7 Panel Level Melt Front Advancement Contours
(a) Below Die   (b) Above Die

With the successful validation of the simulation, the simulation matrix as shown in Fig.1 was then studied for a comprehensive assessment of the process, design and material to enhance molding performance.

3. Systematic Evaluation of the Impact of Process and Design Parameters on Molding for a More Balanced Melt Front and Minimizing Void Issues

We have developed a systematic approach to address the complex flow issues. As the full panel bumped array of flip chip devices would require high computational resources (~7million meshes) compared to chip level study (~500,000 meshes), an initial simplified chip level simulation is used to study the effect of various package-scale parameters. This analysis provides a prediction of the void location and an insight on the key parameters to minimize the voiding problems, and overall minimize the cycle time required to obtain the results.
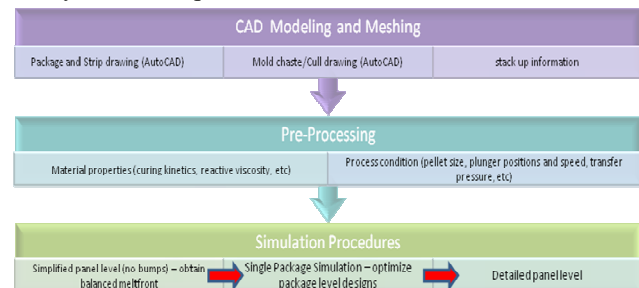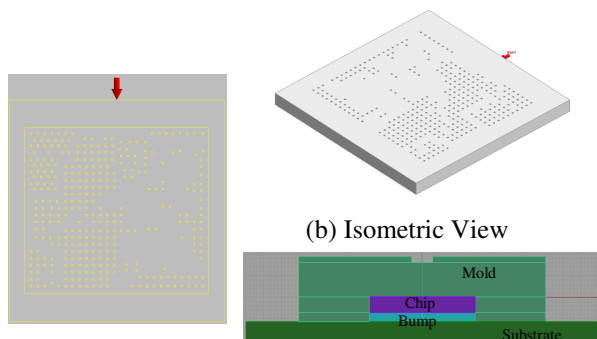

Fig. 8 Flow Chart Illustrating the Systematic Evaluation of the Impact of Process and Design Parameters on Moldability using Molding Simulation Tool Moldex3D

A. Chip Level Simulation

A simplified package 3D model with bumps is first created for an initial analysis as shown in Fig.9, with the mold filling direction as indicated by the red arrow.

(b) Isometric View

(a) Top WireframeView (c) Side View

Fig. 9 Chip Level Simulation Model

The process parameters such as filling time and mold cavity temperature are first varied to analyze the impact of process parameter change on the molding performance using the molding simulation tool. The filling time was varied in the following two key ranges; 0.5s, 1s, 2s (much below gel time) and 10s, 20s, 30s (near gel time). The results as shown in Fig. 10 show that when the filling time is varied in the range much lower than the MUF gel time, the change from 0.5-2s results in minor impact on the void location. This may be due to the minor change in viscosity during this time range (Fig.5) and hence the minor impact on void locations. When the filling time is varied in the range near the MUF gel time, the voiding location varies, for this case shifting closer to the gate side. This could be due to the sharp change in viscosity near the gel time (Fig.5) and with the rapid change in viscosity, a more significant impact on void locations is observed. The results will vary based on the molding material used.
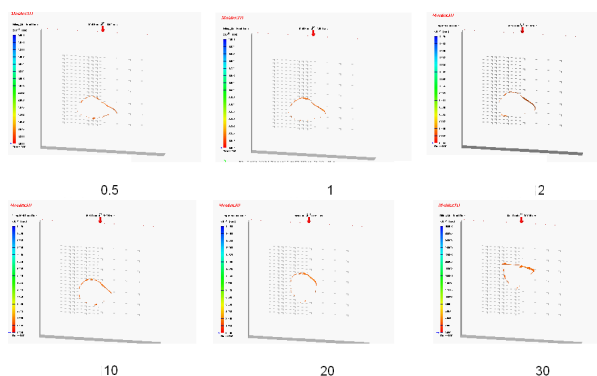

Fig. 10 Impact of Filling Time (s) on Void Location

The mold temperature was varied in the following range: 130°C, 150°C, 170°C, 190°C, 210°C. For this analysis, the filling time is 2s. The results as shown in Fig. 11 show that when filling time is in the range much lower than the MUF gel time, the change from 130°C - 210°C results in minor impact on the void location. This may be due to the minor change in viscosity during this time range, even as the temperature changes from 130°C - 210°C. The results may vary with different material and filling time used.
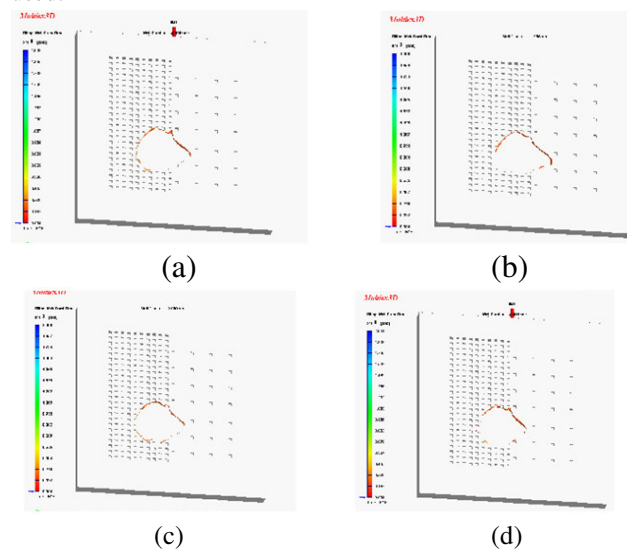

(a) (b)

(c) (d)

Fig. 11 Impact of Mold Temperature on Void Location, a) 130°C, b) 150°C, c)170°C, and d)190°C

Next, the impact of different die thickness keeping the bumps and total package height constant to conducted to study the impact of different gap sizes above and under the die on melt front. As shown earlier in Fig.7, initially, the melt front of the mold top side and bottom side are similar, but due to the presence of bumps, the layout and different in gap sizes between the die top to the mold cavity and bump height, the melt fronts above and underneath the die are separated. The melt front near the top side of mold cavity is much faster than that of the bump area of near the substrate side. The preliminary results indicate that the flow imbalances are potential key factors of void trapping where the two separated melt fronts are merged again. Due to the clearance difference above and under the die, larger flow lag is observed under the die, and we will like to investigate if voids issues reduced by creating better flow balance. Hence, two different die thicknesses as shown in Fig. 12 and Fig. 13 are studies to analyze the impact of similar gap sizes above and under the die on melt front.
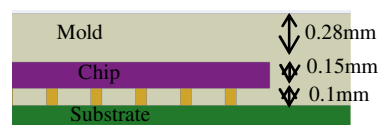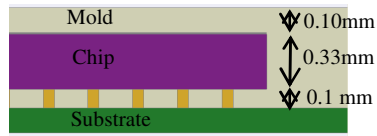

Fig 12: Chip Thickness of 0.15mm

Fig 13: Chip Thickness of 0.33mm

The cross section planar cut is shown in Fig. 14 and the results of the cross sectional melt front advancements for both the thin and thick dies are shown in Fig 15 and Fig 16. The results show that the balancing the flow resistance by decreasing the gap from die top to mold cavity resulted in a more balanced melt front above and underneath the dies, reducing the voiding issues caused where the two separated melt fronts are merged again.
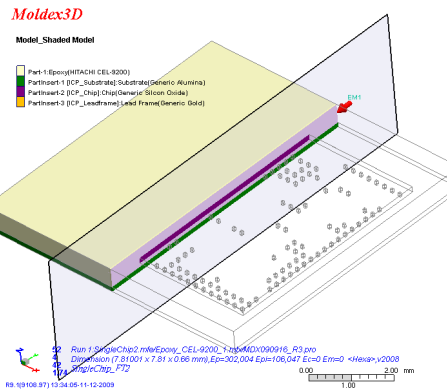

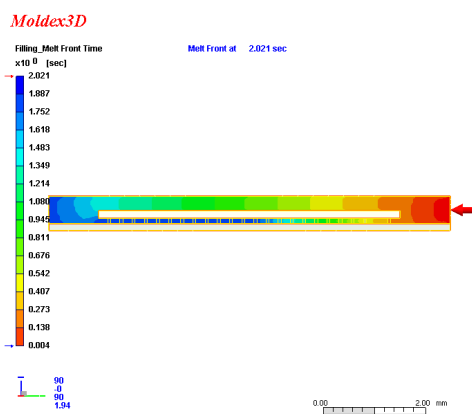Fig 14: Cross Sectional Planar Cut for Analysis

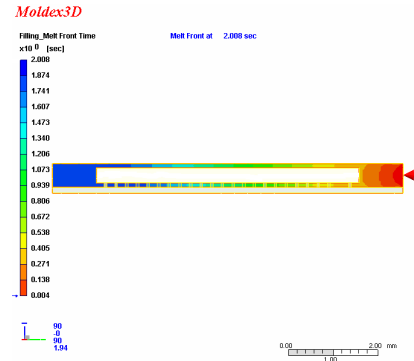Fig 15: Melt Front Profile for Chip Thickness of 0.15mm

Fig 16: Melt Front Profile for Chip Thickness of 0.33mm

We also varied the bump layout to analyze the impact of different bump pitch and layout on the void locations, keeping the die thickness, bump height and total package height constant. In Fig 17, Pitch Array A has the denser bump area with pitch of approximately 0.1mm and the less dense bump area with pitch of approximately 0.6m. The results as shown in Fig 18 indicate that the different bump layout influences the location of the voids trapping. With the denser bumps area located next to the less dense bumps areas, the flow resistance caused by the denser bumps resulted in the shifting of void locations to the area with the denser bump layout. In comparison, when the bumps are evenly distributed, the void location is more centralized, though neared to the vent side with higher viscosity towards the end of filling affecting the void process.
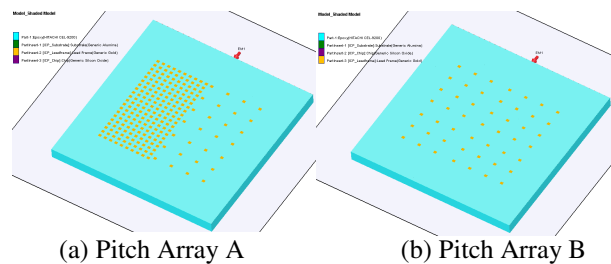

(a) Pitch Array A   (b) Pitch Array B
Fig 17: Different Bump Layout Simulation Models
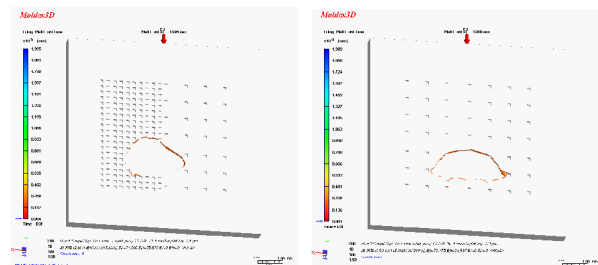

(a) Pitch Array A   (b) Pitch Array B
Fig 18: Void Locations for Different Pitch Arrays

The bump height is also varied to analyze the impact of different bump height on the void locations, keeping the die and mold thickness constant. As shown in Fig 19, two different bump heights were evaluated; 0.1mm and 0.06mm, shown in Fig 19(a) and Fig 19(b) respectively. The bump layout used is Pitch Array A as shown in Fig 17(a). The results as shown in Fig 20 and Fig 21 indicate that the bump height has an impact on the location of the voids trapping. With the smaller bump height of $60\mu m$ while keeping the other factors constant, the flow resistance of the bump area near the substrate side is increased compared to the larger smaller bump height of $100\mu m$. Hence the melt front separation for the device with smaller bump height of $60\mu m$ above and underneath the die is more pronounced. The melt front near the top side of mold cavity is much faster than that of the bump area of near the substrate side when bump height is smaller, resulting in voids trapped nearer to the gate side where the two separated melt fronts are merged again.

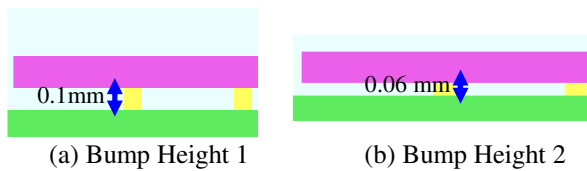(a) Bump Height 1   (b) Bump Height 2

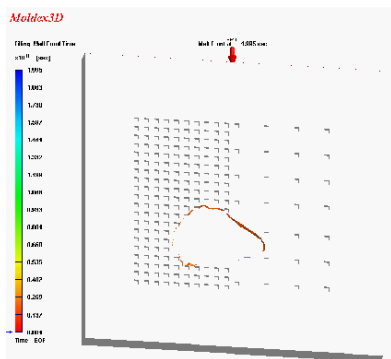Fig 19: Void Locations for Different Bump Height

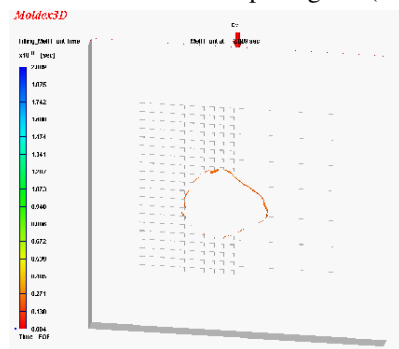

Fig 20: Void Locations for Bump Height 1 (0.1mm)

Fig 21: Void Locations for Bump Height (0.06 mm)

With the insights provided by the preliminary study, the full panel level study is conducted next with the aim of obtaining a balanced melt front and minimizes voids in the most efficient way.

B. Panel Level Simulation

The panel level simulation model is shown in Fig. 23. The total number of finite element meshes used for full panel 3D model for the current study is about 7 million, compared to 500,000 meshes for the chip level study. Analysis was also conducted to ensure that the trends for the single chip are representative of panel level studies for this selected test vehicle and conditions. From our findings, the identified trends of the single chip analysis are representative and insights useful for the subsequent full panel analysis for this test vehicle under the investigated conditions.

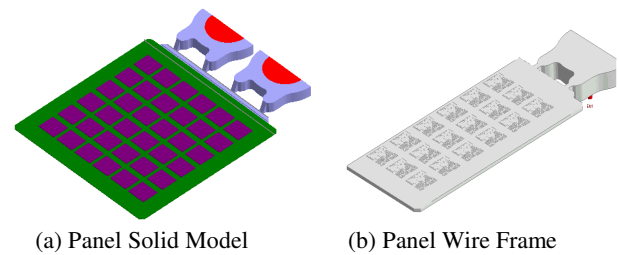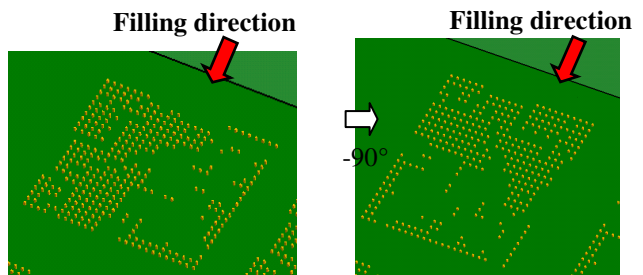(a) Panel Solid Model   (b) Panel Wire Frame Model

Fig. 22 Panel Level Simulation Model Isometric View

For the panel level analysis, we varied the chip orientation and study its impact on the void location for this test vehicle. Two different chip orientations were analyzed as shown in Fig. 24 (a) and (b).

(a) Chip Orientation A   (b) Chip Orientation B

Fig. 23: Panel Level Simulation Model for Different Chip Orientation

The results of the two different chip orientations on the melt front advancements and potential void locations are shown below in Fig 23, Fig 24 and Fig 25. From the results, we observed that different chip orientation resulted in different mold filling trends. For chip orientation A, the denser bump area on the right resulted higher flow resistance, where the melt fronts merged at the area of the denser bumps area, and the potential

voids location shifting towards the denser bump area. For chip orientation B, the denser bump area on top towards the gate side resulted in flow retardation at that area and melt fronts merging nearer to the center of the chip compared to the chip orientation A where the voids are located nearer to the vent side. The results are also shown both for the panel view for both chip orientations as shown in Fig 24 and Fig 25.
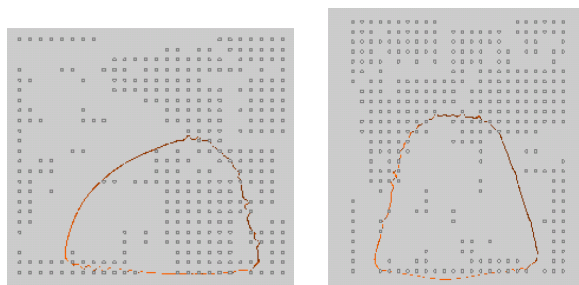
(a) Chip Orientation A   (b) Chip Orientation B
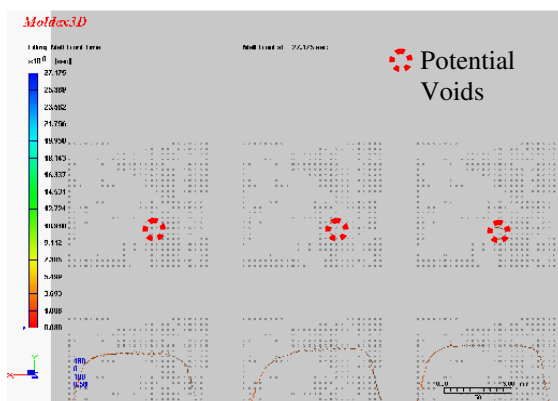Fig. 23: Melt Front on a Package on the Panel for Different Chip Orientation

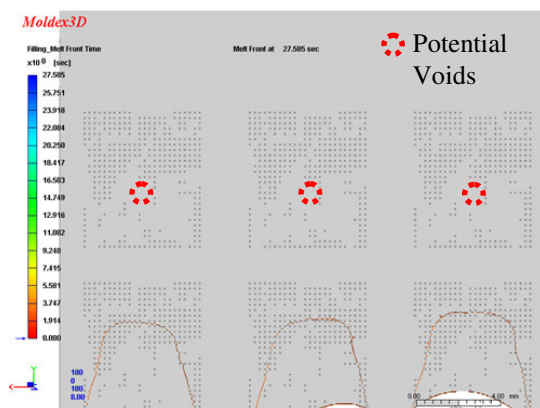Fig. 24: Melt Front on First Two Rows on the Panel for Chip Orientation A

Fig. 25: Melt Front on First Two Rows on the Panel for Chip Orientation B

4. Conclusions

This paper has demonstrated our 3D mold flow modeling capability of the transfer molding process for flip chip devices with MUF using Moldex3D V10. The full MUF rheokinetic behaviors and other material properties were characterized for the flow modeling. The full panel molding simulation was conducted and compared with actual voids locations captured by SAT machine and short shots. The mold filling simulation showed good correlation of the mold fronts obtained by process short shots and actual void locations. With the successful validation of the simulation capability, the tool is then applied to optimize design and process parameters to enhance flow balance, reduce voiding problems and device defects.

To address the complex flow issues with multiple interactive factors, we designed a systematic approach to tackle the problems. An initial simplified chip level simulation is used to provide insights on the key parameters to minimize void problem. With the insights provided by the preliminary study, the full panel level study is conducted next to evaluate the impact of process and design parameters with the aim of obtaining a balanced melt front and minimize voids. Such an approach will reduce the computational resources and total cycle time required to provide mold flow solutions.

From the rheokinetic flow modeling of MUF process, we identified the key factors and minor factors on void trapping simulation results from the extensive list of process and design parameters for this study; including filling time, mold temperature, different gap sizes above and under the die, bump pitch, bump layout, bump height and chip orientation. These insights can be used as upfront guidelines to predict and reduce potential product defects and failures.

With consideration of process, materials and design, we have demonstrated that mold flow simulation is an effective tool to reduce the design-to-implementation cycle time with identification of potential void and melt front imbalance issues. With our increasing range of flip chip products provided, we provide a comprehensive closed-loop solution including moldflow, materials, process, thermal, mechanical and electrical studies [3] to address the rising challenges faced with greater consumer demands for better performance and greater functionalities.

References

1. Zhuqing Zhang and C. P. Wong, "Recent Advances in Flip-Chip Underfill: Materials, Process, and Reliability" IEEE Transactions on Advanced packaging, Vol. 27, No. 3, pp 515-524, 2004.

2. Min Woo Lee, et. al. "A Study on the Rheological Characterization and Flow Modeling of Molded Underfill (MUF) for Optimized Void Elimination Design," Proceedings of the 2008 Electronic Components and Technology Conference (ECTC), Lake Buena Vista, Florida, May 27-30, pp. 382-388, 2008.

3. Siew Hoon Ore, Edith Poh S W, Dr. W.H. Zhu, Dr W.L. Yuan, Dr Nathapong Suthiwongsunthorn, "Co-Design for Thermal Performance and Mechanical Reliability of Flip Chip Devices", Proceedings of the 2010 Electronic Packaging Technology & High Density Packaging (ICEPT-HDP), Aug 16-19, pp. 81-87, 2010.

4. Nguyen, L.T, "Reactive Flow Simulation in Transfer Molding of IC Packages," Proceedings of the 1993 Electronic Components and Technology Conference (ECTC), Orlando, Florida, Jun 1-4, pp. 375-390, 1993

5. M.R. Kamal and M.R. Ryan, "Injection and Compression Molding Fundamentals," chap. 4, A.I.Isayev (Ed.), Marcel Dekker, 1987.

6. M.R. Kamal and M.R. Ryan, "Reactive Polymer Processing: Techniques and Trends,' Advances in Poymer Technology, 4, pp. 323-348, 1984.

7. J. M. Castro, and C. W. Macosko, ''Kinetics and Rheology of Typical Polyurethane Reaction Injection Molding Systems,'' SPE Technical Paper, Vol. 26, pp. 434–438, 1980.